Multistep Molecular Dynamics Simulations Identify the Highly Cooperative Activity of Melittin in Recognizing and Stabilizing Membrane Pores.

Sun, Delin; Forsman, Jan; Woodward, Clifford E

Published in:
Langmuir

DOI:
10.1021/acs.langmuir.5b01995

2015

Multi-Step Molecular Dynamics Simulations Identify the Highly Cooperative Activity of Melittin in Recognizing and Stabilizing Membrane Pores

Delin Sun,[†] *Jan Forsman*,[‡] *and Clifford E. Woodward*[*, †]

[†]School of Physical, Environmental and Mathematical Sciences, University of New South Wales, Canberra ACT 2600, Australia

[‡]Theoretical Chemistry, Chemical Centre, Lund University, P.O. Box 124, S-221 00 Lund, Sweden

ABSTRACT The prototypical antimicrobial peptide, melittin is well known for its ability to induce pores in zwitterionic model lipid membranes. However, the mechanism by which melittin accomplishes this is not fully understood. We have conducted all-atom and coarse-grained molecular dynamics simulations which suggest that melittin employs a highly cooperative mechanism for the induction of both small and large membrane pores. The process by which this peptide induces membrane pores appears to be driven by its affinity to membrane defects via its N-terminus region. In our simulations, a membrane defect was deliberately created through either lipid flip-flop or the reorientation of one adsorbed melittin peptide. In a cooperative response, other melittin molecules also inserted their N-termini into the created defect thus lowering the overall free energy. The insertion of these peptide molecules ultimately allowed the defect to develop into a small transmembrane pore, with an estimated diameter of ~1.5 nm and a lifetime of the order of tens of milliseconds. In the presence of a finite membrane tension, we show that this small pore can act as a nucleation site for the stochastic rupture of the lipid bilayer, so as to create a much larger pore. We found that a threshold membrane tension of 25 mN/m was needed to create a ruptured pore. Furthermore, by actively accumulating at its edge, adsorbed peptides are able to cooperatively stabilize this larger pore. The defect mediated pore formation mechanism revealed in this work may also apply to other amphipathic membrane-active peptides.

KEYWORDS: Antimicrobial peptides; Molecular simulations; Membrane pores; Free energy calculations

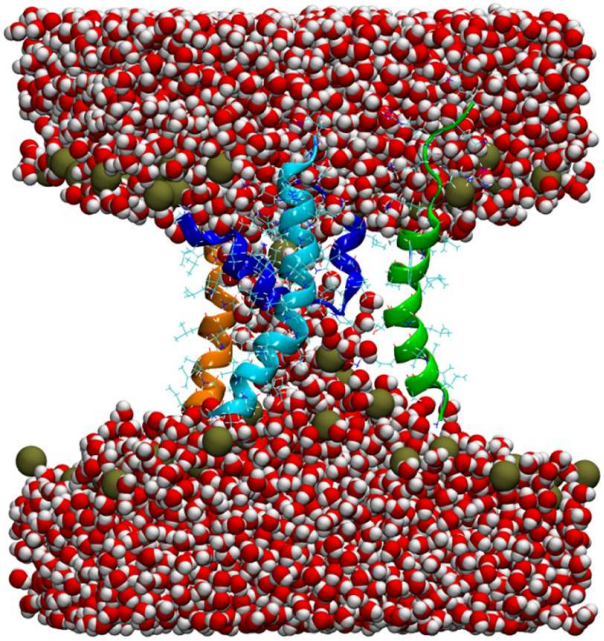

GRAPHIC ABSTRACT

1. INTRODUCTION

Elucidating the underlying mechanisms by which antimicrobial peptides are able to damage eukaryotic and prokaryotic cells is fundamental to the future development of safe and effective antibiotics. Melittin is one of the most extensively studied antimicrobial peptides to date.[1] Over the last few decades, a wealth of information accrued with a variety of methods, has demonstrated that melittin disrupts lipid membranes by generating nanoscale pores.[2-6] However, the exact molecular process by which melittin is able to induce and stabilize such pores remain ambiguous.

Experimental kinetic studies suggest that membrane pore formation is accompanied by melittin translocation across the lipid bilayer.[6] The shape of the membrane pore is toroidal,[7] characterized by lipid heads lining the pore together with a small number of melittin molecules. At low peptide concentration, the pore lifetime has been estimated at less than 10 milliseconds, with graded leakage of vesicle entrapped fluorescent dyes.[6, 8] On the other hand, at higher peptide concentration, Benachir and Lafleur reported an all-or-none type of leakage kinetics. [3]

The direct translocation of individual melittin molecules through lipid membranes without pore formation seems unlikely, with the free energy for this process predicted to be in the range of 27-37 k_BT,[5] using experimentally determined hydrophobicity scales. [9-11] Huang and co-workers, using X-ray diffraction and oriented circular dichroism studies, have proposed a cooperative "two-state" model to explain how melittin stabilizes membrane pores.[12] In this model, melittin initially adsorbs in an α-helical conformation onto the outer leaflet of the lipid bilayer with its axis parallel to the bilayer surface (S-state). According to the model, accumulation of peptide on the bilayer causes thinning and generates membrane stresses such that, above a threshold adsorption concentration, a large pore will become thermodynamically stable. Simultaneously, a fraction of the membrane-bound melittin molecules will change their orientations to become perpendicular to the membrane surface (I-state) presumably as they enter (and stabilize) the newly formed membrane pore. The

resultant stabilized pore is relatively large (with an inner diameter of ~4 nm),[5] which allows the persistent leakage of vesicle-entrapped fluorescent dyes. Hence, the two-state model of Huang and co-workers' would appear to support an all-or-none mode for the release kinetics of melittin, at least above the threshold adsorption concentration. Surprisingly, the experimental studies by Huang *et al*. have also found that melittin peptide was able to distribute itself on the inner leaflet of the lipid bilayer, prior to the formation of the large membrane pore.[5] This intriguing finding is reminiscent of the behaviour of cell penetrating peptides, and suggests that melittin induces small transient pores before the apparent rupture of the lipid membrane to form the larger pores. Peptides adsorbed on the outer (and inner) leaflets appear to expand the membrane, at constant vesicle volume, as seen in experiments.[4] The subsequent opening of a large pore then allows water influx, causing vesicle volume expansion at constant area.[4] The adsorption of peptide changes the optimal area per lipid in the monolayers of the inner and outer leaflets, giving rise to a number of possible mechanisms that can facilitate pore formation. For example, adsorption of melittin on the outer leaflet would give rise to a lateral pressure gradient across the bilayer and induce a tendency for the membrane to change its curvature. The corresponding increased tension on the inner leaflet may initiate pore nucleation there[13]. This mechanism may facilitate the formation of small pores and allow the initial transport of melittin from the outer to the inner leaflets. Once equilibration of melittin adsorption on both leaflets occurs, the surface tension of the bilayer as a whole is zero, as is the preferred bilayer curvature. However, the change in the preferred curvature on each leaflet (due to peptide adsorption) may be responsible for nucleating pores instead.

Notwithstanding the significant and valuable information gleaned from experimental studies, the specific molecular details of small (transient) and large (stable) pores, as well as the potential link between them are not yet fully understood. Molecular dynamics (MD) simulation provides a powerful adjunct to experimental investigations in determining plausible mechanisms for the activity of pore-forming antimicrobial peptides, giving rise to valuable insights. Indeed, some MD

simulations have asserted that melittin can rapidly generate pores in lipid bilayers within a few hundred nanoseconds [14, 15] or a few microseconds.[16] It is not clear to what extent observations of rapid pore formation in simulations is dependent upon the force field used or the initial configuration of the system. Below, we report the results of all-atom MD simulations of high concentrations of melittin peptide (and counterions) interacting with a zwitterionic bilayer made up of dipalmitoylphosphatidylcholine (DPPC) lipids. In our case, we used a different force field and/or a different initial set-up to what was done in earlier work [14, 15] and we did not observe spontaneous pore formation within 400 ns. Instead, we used umbrella sampling to investigate the free energy cost of pore formation in the presence of the melittin. We also carried out unconstrained simulations using all-atom and coarse-grained force fields to investigate the effect of melittin on the properties of the bilayer, and the response of the peptide to membrane pores. These simulations will present a detailed description of the activity of melittin on lipid membranes and illustrate how melittin is able to recognize and cooperatively stabilize membrane defects and pores. These properties would appear to be critical to the way that this peptide is able to disrupt membranes. Our results are summarized in the form of a general model for melittin penetration through lipid membranes.

2. METHODS

We employed the all-atom CHARMM[17] and coarse-grained MARTINI[18, 19] force fields in our simulations. The zwitterionic DPPC lipid bilayer was used as the model membrane as most experimental studies have investigated the pore-forming activity of melittin with zwitterionic lipid bilayers.[4, 5] Interestingly, anionic lipids have been shown to attenuate the activity of melittin.[3, 20] We used both umbrella sampling and unconstrained MD simulations to study the effect of melittin on the DPPC membrane via an overall process, which was partitioned into four distinct steps. The details of the simulation protocols used in each of these steps are described as follows.

2.1 The First Step. In the first step, we considered the influence of the membrane-bound melittin peptides on the structural properties of the bilayer. This was studied using unconstrained, all-atom MD simulations. The model system contained 128 DPPC lipids, 4 melittin peptides (each peptide carries a +5 net charge), 5980 TIPS3P water molecules and 20 chloride ions. The peptide to lipid ratio (P:L = 1:32) falls within the range, of reported experiments, which spans 1:200 to 1:15,[4] and no extra salt was added into the simulation system. The initial configuration consisted of four identical melittin monomers (extracted from the melittin tetramer, PDB code: 2MLT) with an α-helical configuration embedded into the glycerol regions of one leaflet of the bilayer, with their helical axes *parallel* to the bilayer surface. This initial arrangement of the melittin in the lipid bilayer (insertion depth and orientation) was in accord with the X-ray diffraction data of Hristova *et al*.[21] It should be noted that the actual process of peptide adsorption onto the bilayer occurs over a period of milliseconds and is hence quite slow on a molecular timescale.[22] However, the binding free energy of melittin to a zwitterionic bilayer surface has been estimated to be approximately -13 k_BT [23] and so, once they diffuse there, the peptides should essentially remain adsorbed on the bilayer. From that initial configuration, we then carried out 400 ns of MD simulations in a semi-isotropic ensemble, wherein the system's volume was allowed to fluctuate independently in the directions parallel and perpendicular to the bilayer. Simulations of the pure DPPC bilayer (64 lipids and 3200 waters) were also carried out for 200 ns in order to ascertain the effect of the adsorbed peptide.

2.2 The Second Step. In the second step, we investigated the free energy of pore formation with umbrella sampling. The classical nucleation theory of pore formation assumes the existence of a critical pore or membrane defect, which has maximum free energy along the reaction path.[24] However, the free energy at the critical defect is expected to be large and hence a thermodynamically rare event. Thus we used umbrella sampling[25] to investigate pore formation for two distinctly different mechanisms; lipid flip-flop and melittin reorientation. The detailed simulation protocols and parameters used in our umbrella sampling simulations of lipid flip-flop were described in previous

work,[26] so we only discuss them briefly here. Specifically, 27 and 30 sampling windows along the reaction coordinate were generated for lipid bilayers with and without membrane-bound melittin, respectively. In the case where the bilayer had adsorbed melittin peptides, we chose a lipid molecule, which was positioned close to one of the adsorbed peptides, and pulled the hydrophilic head from the outer leaflet (with adsorbed peptides) to the bilayer center. Each of the sampling windows along the reaction coordinate was simulated for 50 ns.

For umbrella sampling simulations of melittin reorientation, the reaction coordinate was chosen to be the z-coordinate (perpendicular to bilayer/water interface) of the vector between the centers-of-mass of the first three residues of the N-terminus of melittin (GLY-ILE-GLY-NH_3^+) and the DPPC lipid bilayer. The same reaction coordinate was also used by Irudayam *et al.*[27] (who, incidentally, used a united-atom force field for their simulations). This reaction coordination was chosen to minimize the free energy barrier to pore formation after it was observed that melittin appears to spontaneously insert its N-terminus into a membrane defect. In this case, 24 sampling windows were used along the reaction coordinate and each window was simulated for 180 ns (see Figure S1). In both sets of umbrella sampling simulations, we used the weighted histogram analysis method (WHAM)[28] in the GROMACS package[29] in order to construct the potential of mean force (PMF) profiles and estimate the statistical errors.

In both sets of umbrella simulations a small membrane pore, stabilized by peptides, was formed. We ran 1150 ns of unconstrained simulations in order to investigate the stability of this pore. The inner diameter of the small pore was calculated by counting the number of water molecules inside a small cylindrical volume centered in the pore (see Supplementary Information). In this calculation, we assumed that the density of confined water molecule was the same as that of bulk water. A similar method for determining pore size was also used by Leontiadou *et al*.[30]

Additional umbrella sampling simulations were also performed to calculate the free energy for removing a melittin molecule from the stabilized pore to the inner leaflet of the bilayer. In this case, the reaction coordinate was chosen to be the z-coordinate of the center-of-mass distance between the whole melittin molecule and the DPPC lipid bilayer. We used 15 sampling windows, where each was simulated for 150 ns (see Figure S2).

2.3 The Third Step. In the third-step of our simulations, we established a potential link between the small membrane pores generated in the second step above and the large membrane pores observed in experiments and assumed to result from membrane rupture. We ran a series of simulations, each 50 ns in duration, using a constant surface tension ensemble. In these simulations, surface tensions of various magnitudes were applied to bilayers, which either contained a small pore (as generated in step two above) or did not. The lateral surface tensions applied to bilayers with a pore were: 14 mN/m, 25 mN/m, 28 mN/m, 30 mN/m and 35 mN/m while the values for the bilayer without a pore were: 35 mN/m, 45 mN/m, 55 mN/m, 65 mN/m and 75 mN/m. In these simulations, the perpendicular pressure was held constant at 1 bar.

2.4 The Fourth Step. In the fourth step, we performed MD simulations using the MARTINI coarse-grained force field[18, 19] to study the response of melittin peptides to the large membrane pore, formed in the third step above. This is key to understanding why the large membrane pore remains stable. The coarse-grained simulations contained 1152 DPPC lipids, 55300 water beads and varying numbers of melittin peptides, corresponding to the P: L ratios of 1:144, 1:72, 1:48 and 1:36, together with a sufficient number of counterions to neutralise the system. The coarse-grained simulations themselves consist of two separate stages: a constrained pore adsorption stage (CPAS) and an unconstrained pore stage (UCPS) simulations. In the CPAS, the ruptured membrane pore was artificially stabilized by using the isotropic pressure coupling method, wherein volume fluctuations were carried out isotropically. We simulated this system for 500 ns, which allowed the peptides to

adsorb to the lipid bilayer (with the stable ruptured pore). In the subsequent UCPS simulations, the pressure coupling scheme was switched to semi-isotropic, allowing independent fluctuations in the area parallel and the distance perpendicular to the bilayer. In this case the system was simulated for 1200 ns. More details about the CPAS and UCPS simulations can be found in our previous work.[31]

2.5 Other Simulation Details. All reported simulations were performed using the GROMACS 4.5.5 package.[29] All-atom simulations were run at the temperature of 323 K using a Nosé-Hoover thermostat[32, 33] with a coupling time constant of 0.5 ps. In the unconstrained all-atom MD and umbrella sampling simulations, the system's volume was allowed to fluctuate according to the semi-isotropic pressure coupling method with both lateral and perpendicular pressures (both 1atm) were independently coupled to the Parrinello-Rahman barostat[34] with a coupling time constant of 5 ps and a compressibility of 4.5×10^{-5} bar^{-1}. Periodic boundary conditions were employed. The simulation time step was 2 fs. Of particular note is our implementation of the CHARMM36 lipid models[17] in the GROMACS package. We used cut-offs of 0.9 nm for the Lennard-Jones (LJ) interactions and also for electrostatic interactions. The latter were evaluated using the particle-mesh Ewald (PME) method.[35] As well, a 0.9 nm neighbour list was updated every 10 steps. The calculated area per lipid, bilayer thickness and free energy of lipid flip-flop suggest that this treatment of non-bonded interactions for the lipid is valid (see results). On the other hand, this cut-off distance may also have an impact in protein interactions. Piana *et al.* investigated the effect of a LJ cut-off distance on the CHARMM force field applied to the folding thermodynamics and structural properties of the 35 residue long villin headpiece peptide.[36] They found that a cut-off distance of 0.9 nm had little effect on the calculated properties of the peptide.[36] In the coarse-grained simulations, the temperature was maintained with a Berendsen thermostat [37] at 310 K. The system's pressure was maintained at 1 bar with the Berendsen barostat,[37] using a compressibility of 3.0×10^{-5} bar^{-1}. Non-bonded LJ and electrostatic interactions were both cut-off at a distance of 1.2 nm. To avoid generation of unwanted noise, the standard shift function of GROMACS was used in which both the energy and force

vanished at the cut-off distance. The LJ potential was shifted from 0.9 to 1.2 nm and the electrostatic potential was shifted from 0 to 1.2 nm. The coarse-grained systems were simulated with an integration time step of 30 fs.

3. RESULTS AND DISCUSSION

3.1 Melittin Causes Significant Structural Change in the Bilayer. After the melittin molecules was placed onto the outer monolayer, we carried out unconstrained MD simulations for 400 ns, during which time no spontaneous pore formation was observed in the bilayer. Indeed, free energy calculations using umbrella sampling (reported below) indicate a large free energy barrier to pore formation, suggesting that their spontaneous occurrence within a few hundred nanoseconds is unlikely. Our observations are in contrast to that reported by Sengupta *et al*,[15] who found spontaneous pore formation within 200 ns in MD simulations of a similar model. It should be noted, however, that a united-atom Berger/GROMOS force field combination was used in that work, as opposed to the all-atom CHARMM force field used here. The Berger/GROMOS force-field combination tends to give very strong interactions between cationic residues and zwitterionic lipids,[38] which will cause a partially embedded peptide to be strongly attracted to the distal leaflet. Furthermore, in reference[15], some of the rapid pore-forming scenarios involved cases where the peptide charge was not balanced by added counter-ions. As shown in recent work, non-electro-neutrality may lead to spurious electrostatic attractions across a bilayer, due to the implicit background charge in the Ewald correction[39]. We also note that, even when sufficient counter-ions have been added, periodic boundary conditions may facilitate a local charge separation across the bilayer, which can also drive pore-formation via an electrostatic mechanism, but over a longer time. While this type of charge separation was also possible in our simulations, they did not cause pore formation (within 400 ns). This is somewhat reassuring, as this electrostatic mechanism is a

consequence of periodic boundary conditions, which are obviously not present in experimental systems.

Our simulations did reveal that the membrane-bound melittin peptides caused significant structural change in the lipid bilayer. Figure 1A shows the time evolution of the area per lipid (APL) of the DPPC bilayer, both in the presence and absence of bound melittin. The APL of the pure bilayer fluctuates around 0.63 nm^2, which is close to the experimental value.[40] With membrane-bound peptide (P: L=1:32), the APL increases to 0.72 nm^2 (averaged over the last 200 ns). We note that the APL appears to have reached equilibrium, at least over the last 200 ns. Thus, adsorption of melittin at this concentration increases the APL by approximately 14.3%. Concomitant with an area increase is a thinning of the bilayer. Figure 1B shows the density profiles for the lipid phosphorous atoms along the direction perpendicular to the bilayer surface. We define the average thickness of the bilayer as the distance between the two peak maxima in the density profile. For the pure DPPC lipid bilayer, this distance is 4.12 nm, which decreases to 3.71 nm when melittin peptides are adsorbed onto the bilayer. We note that the outer leaflet distribution profile becomes broader, due to significant ruffling of the outer leaflet following peptide adsorption. This is because membrane expansion and thinning will not occur uniformly through the bilayer, but only in the vicinity of adsorbed peptide molecules. Figure 1C shows the top view of a typical snapshot of the four melittin molecules on the bilayer surface. Firstly, melittin on the lipid bilayer surface can adopt different configurations. We found that three peptides adopt a slightly bent α-helical configuration in which a small kink exists at the position of proline-14 amino acid. One peptide even adopts a very pronounced "V"-shaped configuration with a more dramatic kink point at the proline-14 position. These melittin configurations are consistent with experimental and other simulation studies.[13, 41]Secondly, the peptides tend to aggregate, which is consistent with patchy adsorption. This cooperativity in peptide adsorption is in line with experimental observations[22] and can be explained in terms of edge defects, which occur in the membrane at the periphery of the bilayer regions perturbed by peptide adsorption.

At these edges, hydrophobic lipid tails are exposed to the aqueous solution, due to irregular packing. This can be seen in Figure 1C, where lipids have been largely expelled from the region where the peptides (coloured in green and purple) are adsorbed. The monolayer depression that accommodates the adsorbing peptides is surrounded by a ring of lipids at the edge of the non-adsorbed parts of the monolayer. Aggregation of the peptide reduces the total edge length. This lipid-mediated attraction will be offset by the mutual electrostatic repulsion between positively charged peptides, which is partially screened by the counter-ions. As will be described below, a similar aggregation of melittin acts to cooperatively stabilize membrane pores. Figure 1D shows the average bilayer insertion depths of the 26 amino acid side-chains on one deeply embedded melittin. Those residues local to the C-terminus penetrate to a shallower depth since the C-terminus of melittin contains two cationic lysine and two cationic arginine residues, which firmly anchors the C-terminus in the lipid phosphate regions. The central part of the peptide is embedded deep below the lipid glycerol groups while the N-terminus is located around the lipid glycerol regions. The somewhat bent configuration of melittin that we observe in our simulations is in agreement with electron spin echo envelope modulation experiments.[42] This bent shape reflects the structural flexibility of melittin due to the presence of the proline residue, which may be important for the ability of melittin to generate membrane pores. This mechanism may be quite different to that of other proline-free antimicrobial peptides, like magainin 2.[43]

While we have only simulated a small section of the lipid bilayer, our results do suggest expected characteristics of peptide adsorption and their effect on the bilayer on a larger scale.[4] Following peptide adsorption, the APL adjusts so as to maintain a zero average surface tension in the bilayer. However, the bilayer will now have a preferred curvature away from the outer leaflet. This is driven by the gradient in the average pressure tensor components parallel to the bilayer surface, creating a positive average surface tension, σ, on the inner leaflet, which counters the expansion in the outer leaflet. We estimate this surface tension as

$$\sigma = \frac{1}{2} k_a \Delta A/A \quad (1)$$

where k_a≈240 mN/m is the stretch modulus of lipid bilayer[4] and $\Delta A/A$ is the fractional change in the APL, which gives $\sigma \approx 17.2$ mN/m. This value lies at the upper end of the experimentally measured antimicrobial peptide-induced surface tension, which is in the range of 5-15 mN/m.[44]

In our system, fluctuations in the local APL occur, with commensurate fluctuations of the local surface tension, as determined by Eq.(1). As shown in Figure 1A, our model predicts fluctuations of around 0.1 nm^2 can occur over a time scale of 400 ns, though we expect even larger fluctuations can occur, with a lower probability, consistent with the Boltzmann distribution.

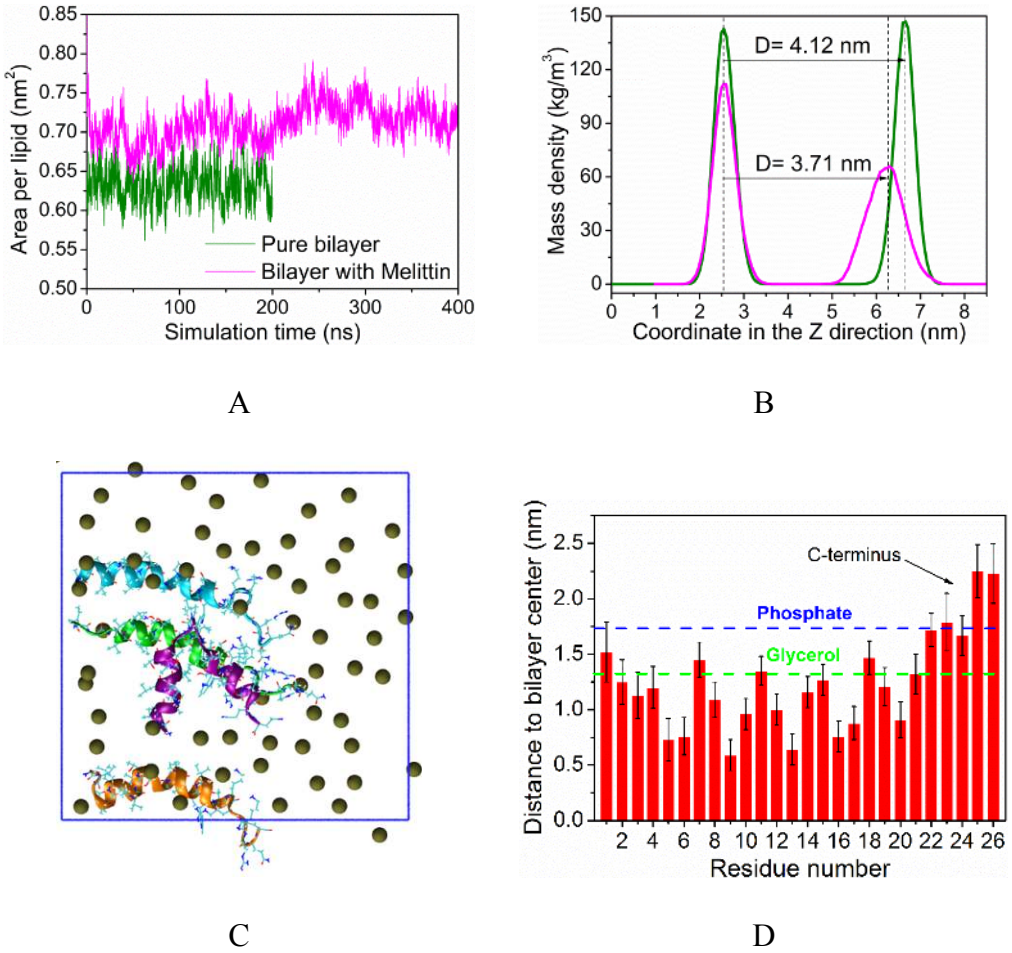

Figure 1. (A) *The time evolution of the area per lipid of the DPPC lipid bilayer with and without membrane-bound melittin peptides. (B) The density profiles for lipid phosphorous atoms along the*

direction perpendicular to the bilayer plane. Green colour denotes the pure DPPC bilayer and pink denotes the DPPC bilayer with melittin peptides. (C) Top view of the aggregation state of 4 melittin peptides on the DPPC bilayer surface. Lipid phosphorous atoms are represented by tan balls. The aggregated peptide molecules (coloured green and blue) occupy a leaflet region largely devoid of lipid molecules. (D) The membrane insertion depths of 26 residues of one deeply embedded melittin peptide. The insertion depth is represented by the center-of-mass distance between the amino acid side chain and the lipid bilayer.

3.2 Transient Pore Formation. As melittin tends to aggregate when adsorbed onto the membrane surface, it is possible that they may act cooperatively to facilitate pore formation as well. In this section, we report the results of simulations of pore formation mechanisms in the presence of adsorbed melittin. We investigated the effect of adsorbed peptide on the free energy cost of short wavelength lipid membrane fluctuations, such as lipid flip-flop and peptide reorientation.

3.2.1 Melittin Facilitates Membrane Defect Formation through Lipid Flip-Flop.

Umbrella sampling simulations were used to create a membrane defect via so-called lipid flip-flop, wherein a single lipid head group is slowly dragged through the membrane. The potential of mean force (PMF) profiles for this process in the pure DPPC bilayer and in the DPPC bilayer with membrane-bound melittin peptides were obtained and compared, see Figure 2A. For the pure DPPC bilayer, we obtained a free energy barrier for lipid flip-flop of 93.1±0.6 kJ/mol. This value is approximately 13 kJ/mol larger than that reported by Tieleman and Marrink,[45] who used the united-atom Berger model for the DPPC lipid. Those authors also observed a trans-membrane pore in the lipid bilayer, when the lipid head was pulled close to the bilayer centre. In our case, a water-filled membrane defect occurred when the lipid was pulled to the bilayer centre, but no pore was observed (see inset Figure 2A). We note that, as in our all-atom simulations, the same LJ cut-off distance of

0.9 nm was used by Tieleman and Marrink.[45] Huang and García have asserted that the Berger lipid model is sensitive to the choice of LJ cut-off distance.[46] They performed simulations using the Berger force field with a 1.4 nm LJ cut-off distance and found that lipid flip-flop did not lead to pore formation in a model DPPC bilayer.[46] They also obtained a lipid flip-flop free energy barrier of approximately 100 kJ/mol, which is close to our result. Hence, the lack of pore formation and higher free energy barrier observed in our simulations (compared to that in reference [45]) appear to be due to the overall stronger attractions between the lipids in the CHARMM force field.

Figure 2A also tells us that the presence of membrane-bound melittin peptides has a marked effect on the PMF for lipid flip-flop. In this case, the simulated free energy barrier is only 64.5±4 kJ/mol, which suggests that the rate of lipid flip-flop would be enhanced by five orders of magnitude (assuming an Arrhenius form for the rate constant). It is worth noting in this context, that a number of experimental studies have concluded that antimicrobial peptide adsorption can induce more rapid lipid flip-flop rates in the bilayers. Fattal *et al*.[47] and Matsuzaki *et al*.[48] attributed the increased rate to a peptide-induced membrane pore, whereas Anglin *et al*.[49] suggest instead that melittin facilitates lipid flip-flop by thinning the bilayer. While our results support the conjecture of Anglin *et al.*, we also find that, in the presence of adsorbed melittin, lipid flip-flop does bring about the formation of a trans-membrane pore. Figure 2A shows that this (small) pore first appears when the lipid head is constrained to lie 0.4 nm away from the bilayer centre. Figure 2B shows a sequence of snapshots from the sampled umbrella window at this lipid distance. Initially, a water-filled membrane defect forms on the outer leaflet, but within 12.5 ns a nearby melittin molecule quickly inserts its N-terminus end into the defect. After 15.3 ns, a second water defect appears in the inner leaflet, which ultimately connects with the first defect, resulting in the trans-membrane pore. After 50 ns in this sampled window, at least one of the melittin peptides has changed its orientation from parallel to the bilayer surface to being perpendicular, as it moves into the pore.

The melittin peptide is able to lower the free energy cost of pore formation by adsorbing strongly to the pore edge. It does this by inserting its hydrophobic residues deep into the lipid chain regions, which are more accessible in the highly curved environment of the pore edges. We have already seen this kind of adsorption in the flat bilayer (Figure 1D). However, in that case, peptide adsorption also serves to create a frustrated bilayer, due to the spontaneous curvature imparted to the outer leaflet by the adsorbed peptide. By migrating peptide to the pore edge, the system lowers the curvature free energy of the bilayer, at the cost of creating a pore. At zero surface tension, the major free energy cost associated with pore formation is the edge free energy of the pore caused by exposure of the hydrophobic lipid components to the aqueous solvent at the highly curved pore edges and the significant steric interactions of the lipid tails at the pore edge. However, the curved interface is more attractive to the peptide than the flat bilayer surface[50] and binding of the peptide to the pore edge effectively lowers the line tension. This description is consistent with the two-state theory presented by Huang *et al*.,[44] as the positive free energy of the frustrated bilayer is essentially equivalent to the "internal membrane tension" described in reference [44].

Once such a pore forms, its radius will fluctuate in size, due to thermal effects. If the pore is stable (or at least metastable) it will fluctuate for some time around an average value. However, if peptide molecules were to diffuse out of the pore, it is likely that the pore would close. We investigate this in the next section.

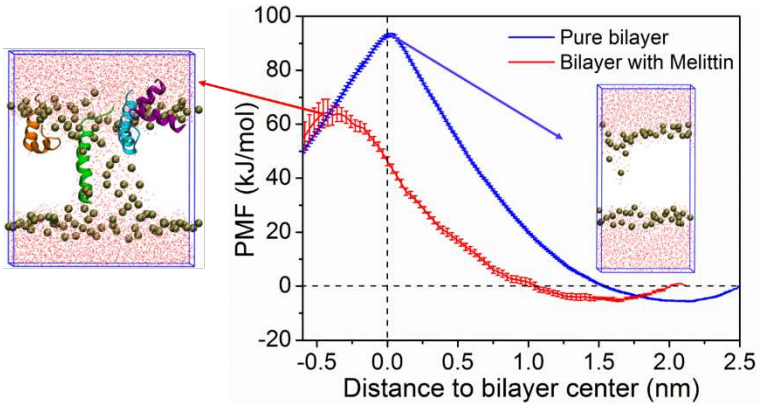

A

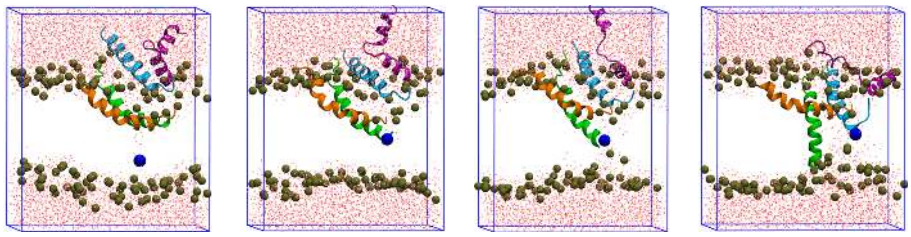

0 ns 12.5 ns 15.3 ns 50 ns

B

Figure 2. (A) *PMF profiles for lipid head flip-flop across the pure DPPC lipid bilayer and the DPPC bilayer with membrane-bound melittin peptides. Error bars indicate the statistical precision. Two snapshots corresponding to the PMF profile maxima are shown after the 50 ns long umbrella sampling simulations. (B) Selected snapshots illustrating the process of melittin insertion into the membrane defect and the development of the defect into a small membrane pore. The constrained lipid phosphorous atom is coloured blue. Lipid tails are not shown for clarity.*

3.2.2 Size, Stability and Lifetime of the Small Membrane Pore. Here we report the results of our investigation of size fluctuations and lifetime of the small membrane pore. To this end, we firstly ran 1150 ns of unconstrained MD simulations starting with the final (50 ns) snapshot shown in Figure 2B. In Figure 3, we show the time evolution of the inner diameter of the small

membrane pore as well as four selected configuration snapshots at 100, 300, 600 and 1150 ns. In the presence of the peptides and without constraints on the lipids, the pore remained open over the full 1150 ns, with the diameter fluctuating around 1.5 nm, which is in agreement with the result reported by Leveritt *et al*.[51] Indeed, it is apparent that during these unconstrained simulations, the system appears to relax, so as to stabilize the pore even further. For instance, after 600 ns all the peptides have diffused into the pore with three of them changing their orientations to become perpendicular to the bilayer surface. Figure 4 depicts one of these perpendicular melittin peptides, and shows the preferred orientation of hydrophobic residues towards the lipid chains, while the hydrophilic residues are directed outwards toward the aqueous phase. The fourth, "V"-shaped melittin molecule cannot fully insert into the pore and remains anchored at the pore mouth via its two positively charged ends. The modelled melittin peptide sequence is NH_3^+-Gly-Ile-Gly-Ala-Val-Leu-Lys-Val-Leu-Thr-Thr-Gly-Leu-Pro-Ala-Leu-Ile-Ser-Trp-Ile-Lys-Arg-Lys-Arg-Gln-Gln-COO^-. The high content of cationic residues on the C-terminus causes it to be firmly anchored at a relatively shallow depth in the outer leaflet. The more hydrophobic N-terminus instead inserts into the pore, which is rich in exposed hydrophobic groups of the lipid. The α-helical structure of melittin is amphipathic and is known to possess the ability to sense packing defects in bilayers via hydrophobic amino acids.[52]

The topological structure of the small membrane pore can be viewed as toroidal, with lipid heads and perpendicularly orientated peptides lining the pore. Our simulated pore structure is very different to the "disordered toroidal pore" reported by Sengupta *et al*.,[15] wherein the melittin peptide adopts randomly tilted orientations. We recall that Sengupta *et al.* employed the Berger lipid and GROMOS protein force fields, which predicts quite strong interactions between the lysine amino acid and zwitterionic lipid heads[38]. This is somewhat inconsistent with experimental interfacial hydrophobicity scales.[53] If the lysine residue close to the N-terminus (Lysine-7) strongly associates with the lipid head groups, the melittin peptide is more likely to tilt at the pore mouth. By contrast, the all-atom CHARMM force field predicts a weak interaction between lysine and the DPPC lipid

heads.[38] Hence, in these simulations, melittin will likely adopt a perpendicular orientation in the pore to maximise hydrophobic contacts within the membrane of the pore surface (as described above).

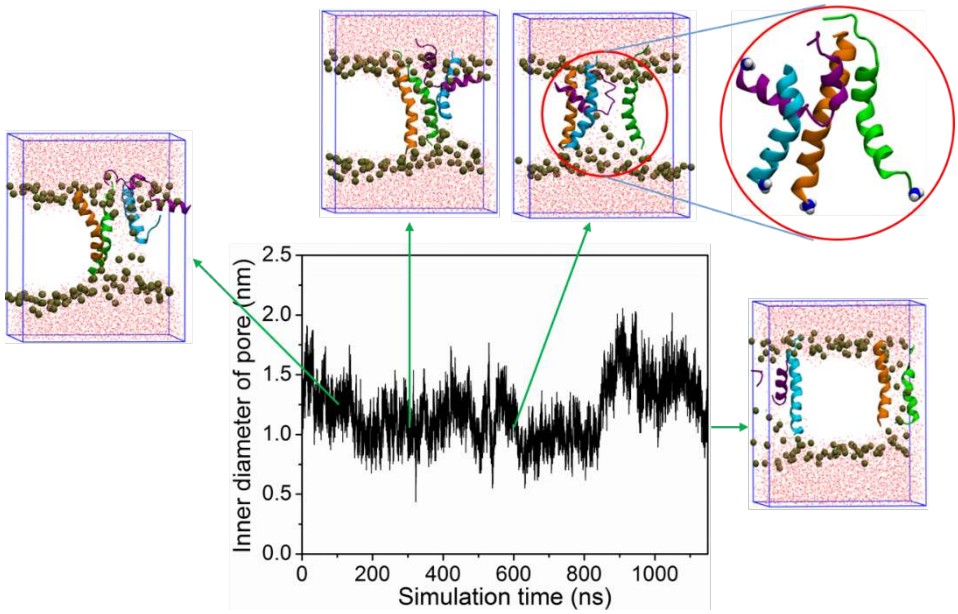

Figure 3. *The time evolution of the inner diameter of the peptide-stabilized small membrane pore. Four selected snapshots at 100 ns, 300 ns, 600 ns and 1150 ns are shown. The snapshot at 600 ns shows that the three perpendicularly orientated melittin peptides all insert their N-termini into the pore.*

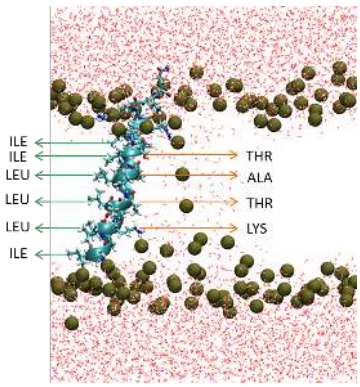

Figure 4. *Orientation of hydrophobic and polar residues of melittin in the pore. Transmembrane residues pointing to the left side (lipid chains) are indicated with green arrows and residues pointing to the right side (membrane pore) with orange.*

In order to investigate the pore-stabilizing role of melittin, we removed the melittin peptides and counterions from our system at the end of the unconstrained 1150 ns MD simulations and continued to run the simulations for a further 100 ns. We found that the pore quickly closed within 20 ns after the peptides were removed from the small pore (see Figure S3). This confirms that pore stability (or at least metastability) requires melittin peptide adsorption and without peptide the pore becomes immediately unstable. It also suggests that the lifetime of the small pore is essentially identical to the time needed for some or all of the peptide to diffuse out of the pore.

To obtain a crude estimate of the lifetime of these pores, we ran umbrella sampling simulations to calculate the free energy profile associated with moving a single melittin molecule uni-directionally through the pore, led by the N-terminus. The PMF profile is plotted in Figure 5. We note that there is a free energy barrier (ΔG_{diff}) for removing the peptide from the pore. This result gives further evidence that the pore is at least metastable. We obtained that ΔG_{diff} = 32.5±7.5 kJ/mol, which is larger than the value of ~5 kcal/mol (and the corresponding diffusion time scale of ~1 ms) assumed in the work of Almeida and Pokorny work.[23] Supposing the peptide diffusion rate is proportional to $\exp(-\Delta G_{diff}/k_B T)$ and that the removal of the first peptide is the rate determining step to pore collapse, we estimate the lifetime of the small pore is of the order of ~80 ms, which is in reasonable agreement with experimental predictions. [6]

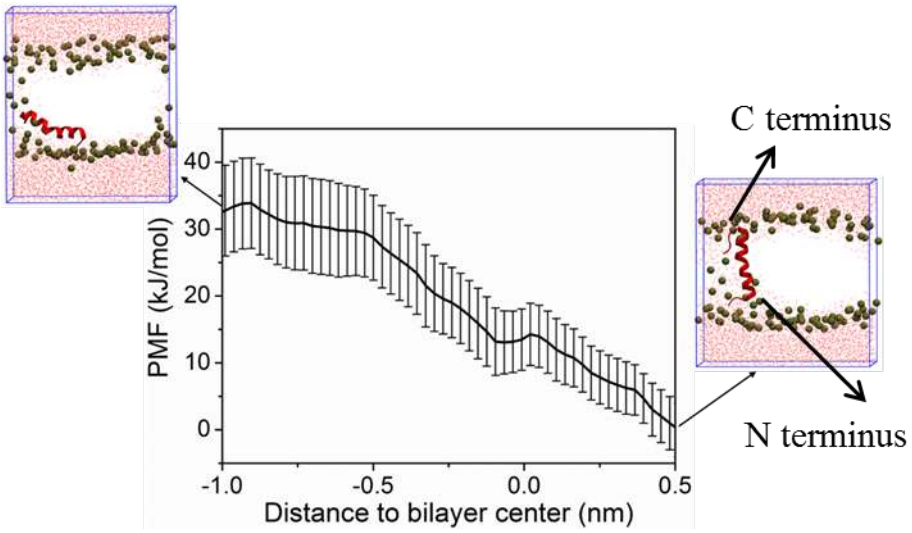

Figure 5. *Potential of mean force for one melittin diffusing out of the small membrane pore. Two snapshots corresponding to the start and end of the reaction coordinate are shown. The other three peptides in the pore are not shown here.*

3.3 Melittin Generates a Small Pore by Reorientating Its N-terminus. The simulations above indicate that melittin reorientates in the small membrane pore by moving its N-terminus towards the inner leaflet of the bilayer. Motivated by this finding, we used umbrella sampling to obtain the PMF associated with reorientation of a melittin peptide, initially embedded on the flat bilayer, so that its N-terminus is pulled towards the bilayer centre. This was carried out for the same system used for the lipid flip-flop simulations described above, by choosing the N-terminus of one of the adsorbed peptides to define the reaction coordinate. Figure 6 shows the resulting PMF profile. The free energy barrier for melittin reorientation across the bilayer is 45±4 kJ/mol, which is approximately 5 kJ/mol larger than that reported by Irudayam *et al.* [27] Those authors used the Berger lipid and GROMOS protein force fields to study melittin reorientation in the zwitterionic lipid bilayer. On the other hand, our result is at least 10 k_BT smaller than the melittin translocation free energies (27-37 k_BT) predicted with experimental hydrophobicity scales.[5] We also note that the free

energy barrier for melittin reorientation is smaller than the value we obtained for lipid flip-flop, which is not surprising, given that the entropic constraints are smaller with the peptide reaction coordinate. We also observed that lipid flip-flop and melittin reorientation generate topologically similar membrane pores (see Figure 2A and Figure 6).

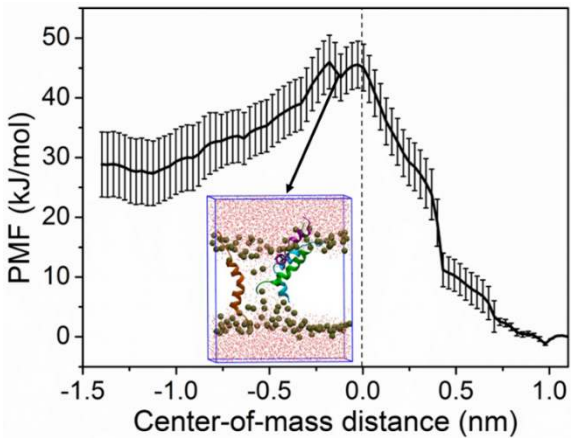

Figure 6. *Potential of mean force for a melittin molecule reorientating its N-terminus across the lipid bilayer. The snapshot shows that melittin reorientation can lead to pore formation and the pore topology is similar to that induced by lipid flip-flop.*

Following Tieleman and Marrink[45], we can approximate the rate of pore formation due to melittin reorientation, assuming

$$\frac{k_f}{k_d} = exp\left(-\Delta G_{pore}/k_B T\right) \quad (2)$$

where k_f and k_d represent the rates of pore formation and dissipation, respectively, and ΔG_{pore} is the activation free energy of pore formation, due to melittin reorientation. From our previous simulations we found that a membrane pore closes quickly (within 20 ns) without adsorbed peptide. We assume a similar rate for the case of pores which dissipate from the activation state (critical pores), to obtain k_d ~10^8 s^{-1}. Using ΔG_{pore}=45 kJ/mol, we obtain k_f ~1.5 s^{-1}peptide^{-1}. Assuming that a giant DPPC lipid vesicle has a diameter of ~50 μm and the P:L ratio is 1:16 on the outer leaflet (the same peptide

concentration as our simulation), the rate of melittin pore formation is estimated as 10^9 s^{-1}. However, this is likely an upper estimate, as it assumes a non-cooperative process of melittin reorientation and permeation, whereas we found that melittin aggregates even in critical pores. This means that our chosen k_d is an overestimate, as critical pore closure still requires diffusion of peptide out of the pore. Using the significantly smaller value of $k_d \sim 10^2$ s^{-1}, which is consistent with our previous calculation on peptide diffusion through a stable pore, an overall pore formation rate in giant vesicles is estimated to be approximately 10^3 s^{-1}. This provides a lower estimate for the pore formation rate, as the critical pore is inherently unstable. Thus, the actual rate is expected to be between these limits. Furthermore, at high peptide density, the total peptide translocation rate may be significantly faster, due to the possibility that peptides may diffuse in a cooperative fashion, as described in recent work due to kinetic rather than thermodynamic stabilization of pores.[26] Notwithstanding the crude nature of the calculation presented here, it does provide plausible support for direct and rapid translocation through small pores as a mechanism for the initial equilibration of the melittin population on both inner and outer leaflets, as suggested by the experiments of Huang *et al*. [5]

3.4 Small Membrane Pores Facilitate Membrane Rupture. As mentioned earlier, experiments indicate that, in the presence of melittin, large membrane pores can stochastically appear in lipid vesicles.[5] More specifically, the experiments show that these large and stable membrane pores will appear above a critical peptide concentration (P:L*).[5] As an example, in the system of melittin with vesicles composed of the diphytanoyl phosphatidylcholine (DPhPC) lipid, the critical concentration is approximately 1:25.[44] According to the two-state theory of Huang *et al*.,[44] pores can increase in size at this critical peptide concentration, as the free energy cost of growing a (peptide stabilised) pore is counter-acted by relieving the "internal membrane tension" free energy, which is assumed to be proportional to $(\Delta A)^2/A$.[44] The quantity $\Delta A/A$ is the fractional change in area upon peptide adsorption and in the two-state model this expansion effectively raises this membrane free energy, analogous to the way an applied surface tension stretches a membrane. As stated earlier, this

membrane free energy can also be described in terms of the curvature free energy of the frustrated bilayer. That is, adsorbed peptide introduces a spontaneous curvature to the bilayer leaflets, which are however forced to remain flat, giving rise to a positive curvature free energy in the bilayer. This observation does not affect the analysis of the two-state model though, as the curvature free energy can be approximately mapped onto an effective long-ranged repulsion between adsorbed peptides, integrated over the bilayer surface, which scales with $(\Delta A)^2/A$. Furthermore, the original analysis in reference[44] did not contain the crucial ideal component to the chemical potential of peptides adsorbed onto the flat layer, which was later rectified. [54]

The small pores described above, result from short wavelength fluctuations of the lipid bilayer, which are opportunistically stabilized by nearby adsorbed peptide molecules. The removal of melittin, which is required for pore closure, exhibits a free energy barrier (see Figures 5 and 6). These pores are expected to form with reasonable rapidity to allow melittin to equilibrate to both sides of the bilayer. Further growth of these small pores will require more melittin (to stabilise the pore rim) and may proceed via a number of possible pathways. For example, adsorbed melittin may diffuse to and insert themselves sequentially into the pore. As seen in Figure 6, the formation of a pore by melittin reorientation exhibits a free energy barrier, even when other peptides are available to help stabilize the pore. The insertion of a melittin molecule into a pre-existing pore with a subsequent increase in the pore radius would presumably encounter a free energy barrier as well and would occur on a time-scale set by peptide diffusion, which may be relatively slow. Another pathway to pore growth, which we explore in this section, is via longer wavelength thermal fluctuations in the bilayer.

As shown in Figure 1A, the APL rapidly fluctuates due to thermal excitations in the system. In the pure bilayer, a local fluctuation in the membrane, which increases the APL significantly, could in principle lead to membrane rupture due to the opening of a pore, but the large free energy barrier

associated with creating a bilayer defect would suppress this process. However, if such a fluctuation occurred in the presence of a small (melittin stabilized) pore of the type described in the previous sections, we would expect that the free energy cost for pore expansion would be considerably lowered. This conjecture is supported by dynamic tension spectroscopy studies on lipid membrane rupture by Evans *et al*. [55] As a result of their experiments, those authors proposed a kinetic model to explain the process of tension-induced membrane rupture. According to the model, membrane rupture starts with the nucleation of a membrane defect and the tension has to rise rapidly enough so that the time needed for traversing the cavitation free energy barrier falls within the lifetime of that membrane defect. Thus, a rapidly applied membrane tension in the presence of a relatively long-lived defect appears essential for rupture of a lipid membrane to form a large pore. Clearly then the small membrane pores (with life-times of the order of milliseconds) can potentially nucleate membrane rupture brought about by membrane fluctuations that cause a rapid increase in the local APL.

To investigate the functional role of small pores in membrane rupture, we performed ten 50 ns long MD simulations in an attempt to rupture lipid bilayers with and without small (melittin stabilized) pores. The effect of a sudden increase in the APL due to membrane fluctuations was mimicked in the simulations by application of a surface tension. The results, given in Figure 7A, show that for the bilayer without pore, a large membrane tension of up to 75 mN/m is still insufficient to rupture the membrane by the end of 50 ns of MD simulations. In contrast, if a small melittin stabilized pore is present, a surface tension of just 25 mN/m is sufficient to cause rapid expansion of the pore (Figure 7B). These results clearly show that the small peptide stabilized pore can act as a potential nucleation site for membrane rupture and large pore formation.

Apart from membrane fluctuations, we conjecture that other (more long-lived) sources of surface tension may occur in this system. For example, as discussed earlier, the adsorption of melittin to

both sides of the bilayer will lead to a frustrated bilayer, wherein the individual leaflets would prefer to have a finite curvature (away from the lipid/water interface). This can be alleviated to some extent by anti-correlated patchy adsorption of melittin, i.e., high peptide concentration on one side of the bilayer is correlated to lower concentration of peptide on the other. This would lead to an undulatory surface with localized curvature, which would lower the membrane free energy to some extent. However, asymmetric peptide adsorption of this type can also induce a localized positive surface tension on the part of the leaflet with less peptide adsorbed. As estimated by Eq. (1) this may be as large as 17 mN/m. Indeed, antimicrobial peptide-induced surface tensions are in the range of 5-15 mN/m.

In the next section we investigate the stability of the large pores. We use larger (coarse-grained) simulations in order to investigate these systems, in order to better represent the types of fluctuations observed in large pores. According to a model by Shillcock and Seifert,[56] the free energy of a membrane pore with low line tension also includes an entropic contribution (S^*) associated with pore shape fluctuations. The pore observed in our simulations has small line tension due to the adsorption of melittin peptides. The S^* term is likely associated with large-scale membrane fluctuation, which occurs stochastically on a giant lipid vesicle and are not captured in the smaller all-atom simulations.

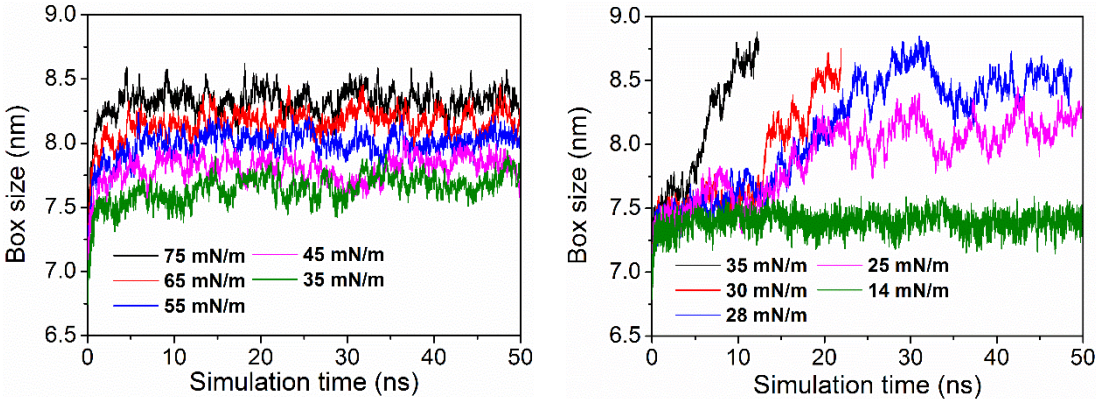

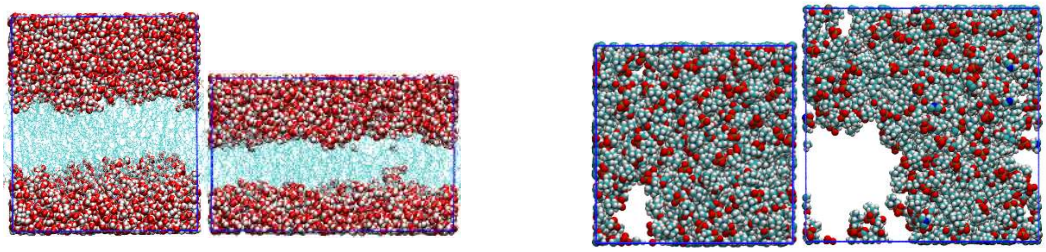

A B

Figure 7. *Time evolution of the size of the simulation box in the XY plane due to the application of a constant surface tension. (A) Case of a lipid bilayer without a peptide-stabilized pore. Side-view of the simulation box before and after application of a large surface tension of 75 mN/m. The membrane does not rupture after 50 ns simulations. (B) Case of a lipid bilayer with an initial peptide-stabilized small membrane pore before and after application of a small membrane tension of 25 mN/m. A top-view of the simulation box illustrates rapid expansion of the membrane pore after 50 ns of simulations. Water and the peptides are not shown for clarity.*

3.5 Melittin Recognizes and Stabilizes the Ruptured Membrane. As shown in the previous section, fluctuations in the APL can lead to rapid growth of pores nucleated by small melittin stabilised pores. In this section we will investigate the fate of such pores using MD simulations. Tamba *et al.* reported that the ruptured membrane pore induced by the antimicrobial peptide magainin 2 was dynamic in character.[57] More specifically, the initially ruptured membrane pores had diameters of some tens of nanometers, then they slowly shrank within minutes to an apparent equilibrium pore state.[57] Wiedman *et al*. reported a similar phenomenon for melittin.[58] High concentrations of melittin induced a rapid burst of leakage of vesicle-entrapped fluorescent dyes. After the initial burst, however, the leakage rate slowed down to zero within ~10 minutes.[58] Here, we use coarse-grained MARTINI model simulations to elucidate the behaviour of ruptured pores in the presence of melittin peptides. The simulated systems are some ten times larger than the CHARMM

all-atom simulations presented above, albeit with a more crude representation of molecular interactions. The simulation protocols were described earlier.

In our CPAS simulations, we initially applied an electric field of magnitude 0.7 V/nm across the DPPC bilayer to create a large pore, rather than application of a surface tension. Melittin peptides and counterions were then added to the surrounding solvent and the electric field removed. An isotropic pressure coupling method, wherein volume fluctuations were carried out uniformly in all dimensions, was then employed. We have shown in previous work that this ensemble keeps the pore open by disallowing independent volume fluctuations in the plane of the bilayer.[31] Figure 8 (A-D) show snapshots at the end of 500 ns of CPAS simulations for varying concentrations of melittin. Consistent with our all-atom simulations, we find melittin has a strong affinity to the membrane pore, due to the non-electrostatic interactions between the hydrophobic residues of the peptide and the lipid tails, also captured in the MARTINI model.[31] The strong affinity of melittin to ruptured membrane pores observed here, may explain the experimental results of Benachir and Lafleur.[3] They found that melittin peptide can distinguish between ruptured and intact lipid vesicles, the peptides prefer to adsorb to ruptured vesicles.

As was the case for the small pores investigated above, it is likely that the binding of melittin to the larger (ruptured) pores also imparts stability to the pores. We tested this hypothesis by using the final CPAS configurations to initiate further UCPS simulations. The latter, unconstrained simulations, ran for 1.2 μs, during which the system's pressure coupling was switched to the semi-isotropic scheme. This ensemble generates an unconstrained tensionless pore. Figure 7E shows that with low melittin concentration, P: L=1:144, the initially ruptured membrane pore almost closes at the end of 1.2 μs of simulations. Our all-atom simulations have shown that just four melittin peptides can stabilize a membrane pore with diameter approximately 1.5 nm. The different result obtained here can be attributed to the large size of coarse-grained water model. It is more difficult for the

larger coarse-grained water to insert into the small pore. When the peptide concentration is increased, the ruptured pore becomes stabilized to a larger size (see Figure 8 (F-H)). An equilibrium pore size that is dependent upon the mellitin concentration is consistent with experiments.[6] We calculated the inner diameter of the equilibrium pore to be 4.7 nm when the P: L ratio is 1:36 (see Figure S4 for the time evolution of the inner diameter of the pore). This result is in good agreement with the experimental value of 4.4 nm reported by Lee *et al*.[5] However, OCD measurements indicate that (on average) only 4-7 melittin peptides are in in a perpendicular (I) orientation in the large membrane pore.[5] Our coarse-grained simulations predict that overall approximately 27 melittin peptides exist in rather random orientations in the 4.7 nm pore. This may explain the discrepancies in peptide number, as OCD measurements determine the average perpendicular projection of the helical axis of the peptides.

While suggestive, the relevance of our simulations to experiments needs further discussion. As the pore is initially constrained in the CPAS simulations, it leaves open the question as to whether peptides in reality have the requisite time to migrate to and bind the pore edges before the latter closes. In the CPAS simulations the melittin was added initially to the surrounding solution. It is plausible that peptides already adsorbed on the bilayer surface, and which are proximal to the pore, may have time to diffuse to the pore edge before closure. The typical time required for adsorbed peptide to reach the pore edge depends upon the peptide surface density and its diffusion coefficient on the bilayer. Furthermore, we note that in Figure 8(F-H) the stabilized pores seem to possess a "halo" of peptides, which are absorbed onto the flat part of the bilayer and distinct from those that are adsorbed on the inside of the pore surfaces. These peripherally adsorbed peptides are unlikely to play as large a role in pore stabilization, but are probably attracted there via aggregation mechanisms discussed earlier. Upon membrane rupture and the formation of the larger pores, these peripheral peptides are then able to insert themselves quickly onto the pore surfaces, leading to their stabilization. Giménez *et al.*[59] recently employed atomic force microscopy (AFM) and observed

circular nanoscale membrane pores in the lipid monolayers when the peptide's concentration was close to our simulation study. However, the AFM observed membrane pore is characterized by the significant protrusion at the pore edge. The protrusion is a sign of peptide aggregation at the pore edge, which is in agreement with our coarse-grained simulation results. While our coarse-grained simulations did not reveal very significant peptide protrusion at the pore edge, it is pertinent to note that the lipid monolayer is significantly thinner than the lipid bilayer. Our coarse-grained simulations indicated that the melittin peptides are fully inserted into the bilayer with a thickness of ~4 nm. The decreased monolayer thickness may expose part of the peptide to the air and consequently a significant protrusion was seen in the AFM image.

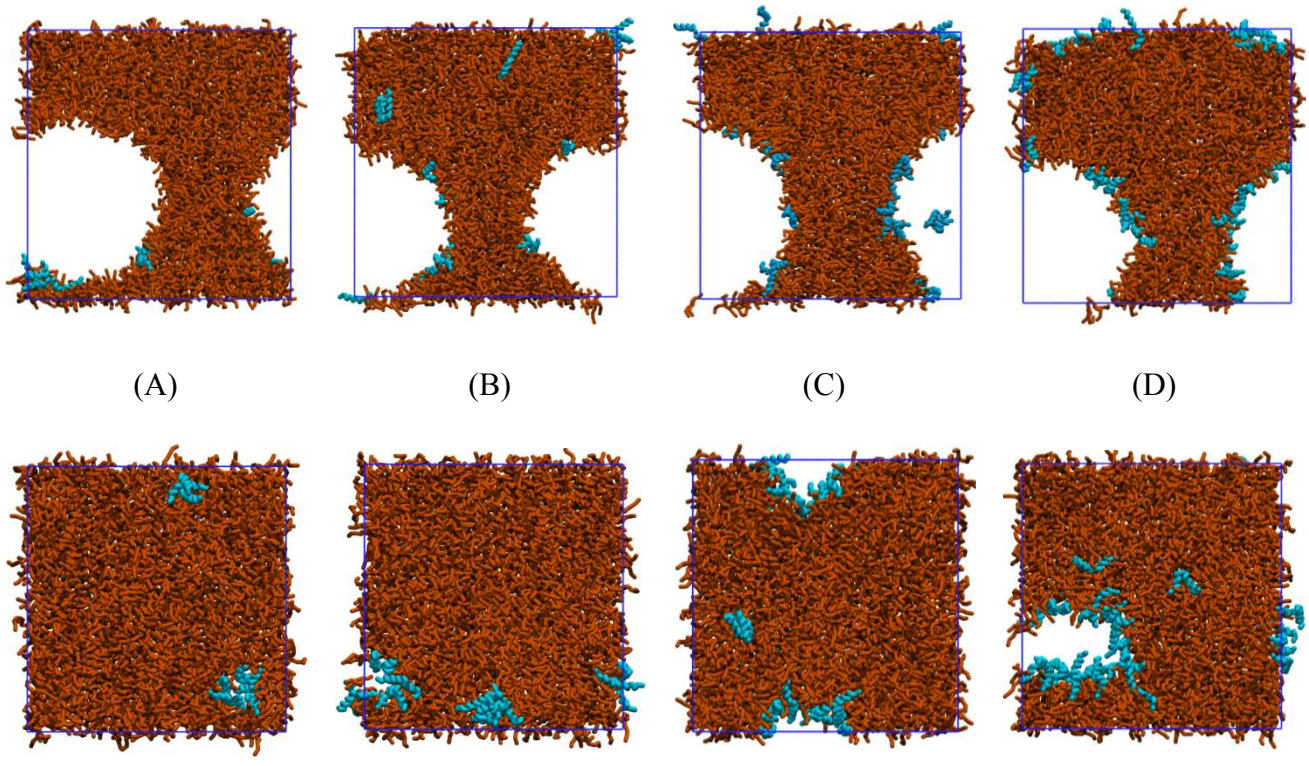

Figure 8. *(A-D) Snapshots derived from CPAS simulations show that melittin prefers to adsorb to the ruptured membrane pore edge. (E-H) Snapshots derived from UCPS simulations show that aggregation of melittin in the membrane pore edge can stabilize the membrane pore. The size of the*

stabilized membrane pore is dependent on the number of peptide (or peptide concentration) in the pore. At P: L=1:36, the inner diameter of the pore is calculated to be 4.7 nm.

In reality, there may be a very large number of rupturing events, the majority of which do not have the right conditions to produce large pores stabilized by adsorbing peptide. However, only a small number of such pores are needed to permit the rapid release of dyes seen in experiments.

3.6 A Model for the Formation of Melittin-Stabilized Membrane Pores. The results of our simulation studies have prompted us to propose the following conceptual model for the formation of melittin-stabilized membrane pores, which is summarized in Figure 9. This has elements which are consistent with the two-state model, already proposed by Huang *et al*.,[44] but is informed and supported by the four simulations steps carried out in this work. The major components of the model are as follows:

(1) Melittin adsorption and accumulation on the lipid membrane surface causes significant surface area expansion and thinning of the lipid bilayer. Our simulations show this is a consequence of deep embedding of the central part of the peptide into the region below the lipid glycerol groups. The melittin peptides show strong evidence of aggregation on the flat bilayer.

(2) Small water-filled membrane defects can be created by mechanisms such as lipid flip-flop or peptide reorientation, corresponding to small wavelength thermal fluctuations. If a defect is formed within or close to a cluster of adsorbed peptides, those peptide molecules, which are in close proximity to the defect, can quickly insert their N-terminus and lend it some stability. We have shown that this stabilization process can be enhanced by cooperative adsorption of the peptides, whereby several melittin peptides are able to develop the membrane defect into a small membrane pore. We found that four adsorbed peptides could create a pore with a diameter of up to 1.5 nm and an estimated lifetime of approximately tens of milliseconds. At a lower peptide density than that

simulated here, we expect even smaller membrane pores could form. These small metastable pores allow rapid diffusion of melittin from the outer to the inner leaflet.

(3) The small pores arise from short wavelength thermal fluctuations that are stabilized by a few adsorbed peptides. Once they are formed, they can act as potential nucleation sites for the sudden rupture of the membrane. Membrane rupture is a stochastic process and is likely caused by longer wavelength fluctuations that bring about a localized increase of the APL. If a nucleating pore is present in the region, it is able to expand rapidly given a sufficiently large membrane fluctuation. Our simulations indicate that this could occur when the surface tension (corresponding to the local increase in the APL) is of the order of 25 mN/m.

(4) As with the small pores, the larger ruptured pores are also stabilized by the cooperative adsorption of the peptides at the pore edges. The peptide has a high affinity to the ruptured pore due to the exposure of the hydrophobic parts of the lipid. Because the pore radius, R_p, will increase as peptide is added to its edge, the free energy of peptide adsorption to the pore approximately scales with the number of peptide molecules adsorbed there. That is, the chemical potential of peptide in the pore is approximately constant (irrespective of pore size). If the peptide chemical potential in the pore is higher than its value on the flat part of the bilayer, the pore is metastable. The metastability arises from the free energy barrier to removal of peptide from the pore (see Figure 5). In this concentration regime the pore will fluctuate between a series of metastable states, with the free energy increasing with size as depicted in Figure 10A.

If the total amount of adsorbed peptide is increased, the chemical potential of the peptide adsorbed to the flat sections of bilayer also increases. That chemical potential contains both ideal and interaction parts. The ideal term increases as ln(P/L). When peptides adsorb on a leaflet there is local distortion of the bilayer. It is thermodynamically favourable for peptides to "share" the membrane distortion, as evidenced by the peptide clustering seen in our simulations, giving rise to patchy

adsorption. On the other hand, the cluster sizes will be limited by internal electrostatic repulsions and clusters will also begin to electrostatically repel each other once they become more numerous. At the critical peptide concentration (P:L*), the chemical potential of the peptide on the flat part of the bilayer has increased to the point where it becomes equal to that in the pore. If the peptide concentration is above this critical value on the flat bilayer, peptide will be added to the pore edges, until equilibrium is re-established. This situation is depicted in Figure 10B, which gives a free energy minimum at this equilibrium point.

This model also explains why one obtains qualitatively different results with experiments on dye efflux from vesicles in the presence of melittin. If the melittin concentration is below P:L*, then the large pores produced by thermal fluctuations remain metastable and hence have a relatively short lifetime, leading to graded release. On the other hand, if the overall peptide concentration is above the critical value, the large pores become absolutely stable and long-lived, leading to all-or-none release kinetics.

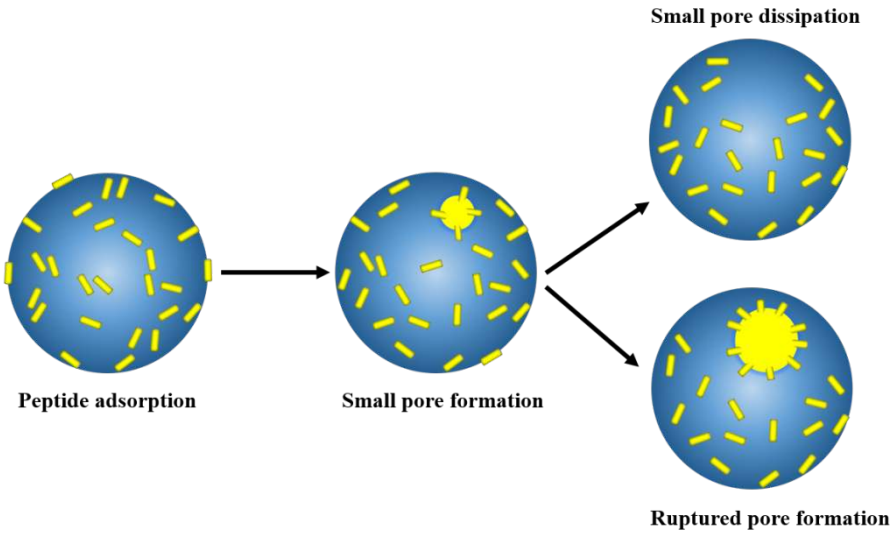

Figure 9. *A proposed model for the process of melittin inducing small and large pores in a lipid membrane.*

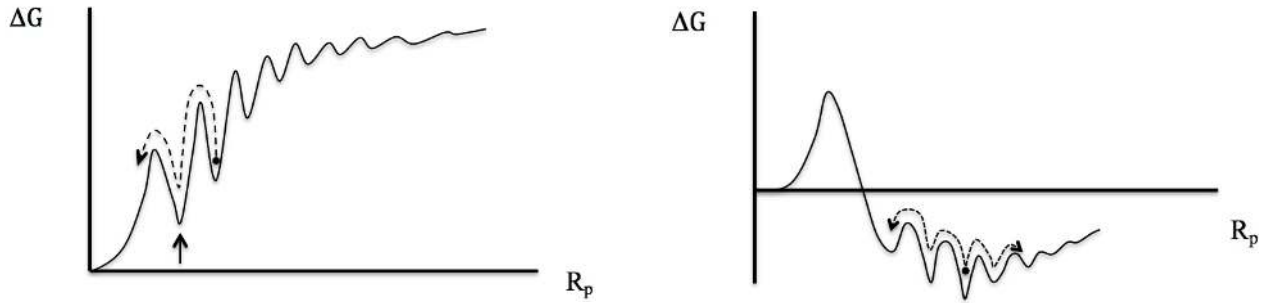

(A) (B)

Figure 10. *(A) Schematic of the free energy vs pore radius for P: L below the critical value. Pore states are metastable. Dashed curve represents pore fluctuations over free energy barriers, corresponding to changes in the number of peptides adsorbed to the pore edge. The first state (marked by the arrow) represents the nucleating pore from which the larger pores are formed via membrane fluctuations. (B) Schematic of the free energy vs pore radius for P: L above the critical value. Here the pore states are more stable than pore free states, provided the peptide concentration adsorbed on the flat part of the bilayer is less than P:L*. If the number of peptides adsorbed at the pore becomes too large, the adsorption concentration on the flat bilayer drops below the critical value and the free energy increases.*

4. CONCLUSIONS

Direct translocation has been proposed as a possible mechanism for melittin penetration, though experimental hydrophobicity scales estimate the free energy barrier for melittin translocation to be in the range 27-37 k_BT.[5] We have performed free energy calculations that estimate the free energy barrier for melittin re-orientating its hydrophobic N-terminus across the lipid bilayer is at least 10 k_BT lower than that predicted by the hydrophobicity scales. This barrier is lowered by the cooperative action of several melittin molecules, which stabilizes a small pore. A similar behaviour is also seen in the case of lipid flip-flop. In the absence of adsorbed melittin, lipid flip-flop is unable to produce

a pore in the DPPC bilayer. This is not the case when melittin is present, whereby the dragging a single lipid to near the centre of the bilayer is able recruit peptide molecules to catalyse pore formation. This suggests a common mechanism whereby melittin peptide is attracted to and stabilizes membrane defects that expose deeper lying hydrophobic groups in the bilayer. This mechanism may explain why melittin can generate ion-leakage pores even when the peptide concentration is very low.[5, 58] We have also shown that small membrane pores of this type can nucleate rupture of the membrane to produce larger pores, via thermal fluctuations causing localized stretching of the bilayer to produce a positive surface tension. Coarse-grained simulations then show that melittin adsorbs strongly to the edge of the ruptured pore and acts to stabilise it. We propose a model, which generalizes the two-state model of Huang *et al.*, to some extent.[44] The "internal membrane tension" free energy associated with peptide adsorption can be identified as the curvature free energy of a frustrated bilayer. This term, due to peptide/peptide interactions, together with the reduction in the line tension of the pore by adsorbed peptide, dictates whether formation of a pore is thermodynamically favourable. However, the pore states themselves are at least metastable, due to the free energy cost of removing peptide molecules from the pore. Finally, we note that in previous work, we found that arginine-rich peptide can also utilize naturally occurring membrane defects to generate pores.[26] Hence, membrane defect recognition and stabilization could be a common mechanism of action for a wide range of membrane-active peptides. Such a mechanism is also supported by other work.[60, 61]

ASSOCIATED CONTENT

Supporting Information

Method to calculate the inner diameter of small membrane pore in all-atom simulations; convergence of PMF for one melittin reorienting its N-terminus across the lipid bilayer; convergence of PMF for

one melittin diffusing out of the small membrane pore; snapshots illustrating the membrane pore closure in the DPPC lipid bilayer; time evolution of the inner diameter of the large membrane pore stabilized by melittin peptides. This material is available free of charge via the Internet at http://pubs.acs.org.

AUTHOR INFORMATION

Corresponding Author

* To whom correspondence should be addressed. E-mail: c.woodward@adfa.edu.au.

Author Contributions

The manuscript was written through contributions of all authors. All authors have given approval to the final version of the manuscript.

ACKNOWLEDGMENT

An allocation time from the Lunarc Computing Center at Lund University are gratefully acknowledged. JF acknowledges financial support from the Swedish Research Council.

REFERENCES

(1) Raghuraman, H.; Chattopadhyay, A. Melittin: A Membrane-Active Peptide with Diverse Functions. *Biosci. Rep.* **2007,** *27*, 189-223.

(2) Allende, D.; Simon, S. A.; McIntosh, T. J. Melittin-Induced Bilayer Leakage Depends on Lipid Material Properties: Evidence for Toroidal Pores. *Biophys. J.* **2005,** *88*, 1828-1837.

(3) Benachir, T.; Lafleur, M. Study of Vesicle Leakage Induced by Melittin. *Biochim. Biophys. Acta Biomembr.* **1995,** *1235*, 452-460.

(4) Lee, M. T.; Hung, W. C.; Chen, F. Y.; Huang, H. W. Mechanism and Kinetics of Pore Formation in Membranes by Water-Soluble Amphipathic Peptides. *Proc. Natl. Acad. Sci. U.S.A.* **2008,** *105*, 5087-5092.

(5) Lee, M. T.; Sun, T. L.; Hung, W. C.; Huang, H. W. Process of Inducing Pores in Membranes by Melittin. *Proc. Natl. Acad. Sci. U.S.A.* **2013,** *110*, 14243-14248.

(6) Matsuzaki, K.; Yoneyama, S.; Miyajima, K. Pore Formation and Translocation of Melittin. *Biophys. J.* **1997,** *73*, 831-838.

(7) Yang, L.; Harroun, T. A.; Weiss, T. M.; Ding, L.; Huang, H. W. Barrel-Stave Model or Toroidal Model? A Case Study on Melittin Pores. *Biophys. J.* **2001,** *81*, 1475-1485.

(8) Rex, S.; Schwarz, G. Quantitative Studies on the Melittin-Induced Leakage Mechanism of Lipid Vesicles. *Biochemistry* **1998,** *37*, 2336-2345.

(9) Hessa, T.; Kim, H.; Bihlmaier, K.; Lundin, C.; Boekel, J.; Andersson, H.; Nilsson, I.; White, S. H.; von Heijne, G. Recognition of Transmembrane Helices by the Endoplasmic Reticulum Translocon. *Nature* **2005,** *433*, 377-381.

(10) Moon, C. P.; Fleming, K. G. Side-Chain Hydrophobicity Scale Derived from Transmembrane Protein Folding into Lipid Bilayers. *Proc. Natl. Acad. Sci. U.S.A.* **2011,** *108*, 10174-10177.

(11) Wimley, W. C.; Creamer, T. P.; White, S. H. Solvation Energies of Amino Acid Side Chains and Backbone in a Family of Host-Guest Pentapeptides. *Biochemistry* **1996,** *35*, 5109-5124.

(12) Huang, H. W. Action of Antimicrobial Peptides: Two-State Model. *Biochemistry* **2000,** *39*, 8347-8352.

(13) Terwilliger, T. C.; Weissman, L.; Eisenberg, D. The Structure of Melittin in the Form I Crystals and Its Implication for Melittin's Lytic and Surface Activities. *Biophys. J.* **1982,** *37* (1), 353-361.

(14) Manna, M.; Mukhopadhyay, C. Cause and Effect of Melittin-Induced Pore Formation: A Computational Approach. *Langmuir* **2009,** *25*, 12235-12242.

(15) Sengupta, D.; Leontiadou, H.; Mark, A. E.; Marrink, S. J. Toroidal Pores Formed by Antimicrobial Peptides Show Significant Disorder. *Biochim. Biophys. Acta Biomembr.* **2008,** *1778*, 2308-2317.

(16) Santo, K. P.; Irudayam, S. J.; Berkowitz, M. L. Melittin Creates Transient Pores in a Lipid Bilayer: Results from Computer Simulations. *J. Phys. Chem. B* **2013,** *117*, 5031-5042.

(17) Klauda, J. B.; Venable, R. M.; Freites, J. A.; O'Connor, J. W.; Tobias, D. J.; Mondragon-Ramirez, C.; Vorobyov, I.; MacKerell, A. D.; Pastor, R. W. Update of the CHARMM All-Atom Additive Force Field for Lipids: Validation on Six Lipid Types. *J. Phys. Chem. B* **2010,** *114*, 7830-7843.

(18) Monticelli, L.; Kandasamy, S. K.; Periole, X.; Larson, R. G.; Tieleman, D. P.; Marrink, S. J. The MARTINI Coarse-Grained Force Field: Extension to Proteins. *J. Chem. Theory Comput.* **2008,** *4*, 819-834.

(19) Marrink, S. J.; Risselada, H. J.; Yefimov, S.; Tieleman, D. P.; de Vries, A. H. The MARTINI Force Field: Coarse Grained Model for Biomolecular Simulations. *J. Phys. Chem. B* **2007,** *111*, 7812-7824.

(20) Ladokhin, A. S.; White, S. H. 'Detergent-Like' Permeabilization of Anionic Lipid Vesicles by Melittin. *Biochim. Biophys. Acta Biomembr.* **2001,** *1514*, 253-260.

(21) Hristova, K.; Dempsey, C. E.; White, S. H. Structure, Location, and Lipid Perturbations of Melittin at the Membrane Interface. *Biophys. J.* **2001,** *80*, 801-811.

(22) Klocek, G.; Schulthess, T.; Shai, Y.; Seelig, J. Thermodynamics of Melittin Binding to Lipid Bilayers. Aggregation and Pore Formation. *Biochemistry* **2009,** *48*, 2586-2596.

(23) Almeida, P. F.; Pokorny, A. Mechanisms of Antimicrobial, Cytolytic, and Cell-Penetrating Peptides: From Kinetics to Thermodynamics. *Biochemistry* **2009,** *48*, 8083-8093.

(24) Xu, X. F.; Ting, C. L.; Kusaka, I.; Wang, Z. G. Nucleation in Polymers and Soft Matter. *Annu. Rev. Phys. Chem.* **2014,** *65*, 449-475.

(25) Torrie, G. M.; Valleau, J. P. Nonphysical Sampling Distributions in Monte Carlo Free-Energy Estimation: Umbrella Sampling. *J. Comput. Phys.* **1977,** *23*, 187-199.

(26) Sun, D. L.; Forsman, J.; Lund, M.; Woodward, C. E. Effect of Arginine-Rich Cell Penetrating Peptides on Membrane Pore Formation and Life-Times: A Molecular Simulation Study. *Phys. Chem. Chem. Phys.* **2014,** *16*, 20785-20795.

(27) Irudayam, S. J.; Pobandt, T.; Berkowitz, M. L. Free Energy Barrier for Melittin Reorientation from A Membrane-Bound State to a Transmembrane State. *J. Phys. Chem. B* **2013,** *117*, 13457-13463.

(28) Souaille, M.; Roux, B. Extension to the Weighted Histogram Analysis Method: Combining Umbrella Sampling with Free Energy Calculations. *Comput. Phys. Commun.* **2001,** *135*, 40-57.

(29) Pronk, S.; Pall, S.; Schulz, R.; Larsson, P.; Bjelkmar, P.; Apostolov, R.; Shirts, M. R.; Smith, J. C.; Kasson, P. M.; van der Spoel, D.; Hess, B.; Lindahl, E. GROMACS 4.5: A High-Throughput and Highly Parallel Open Source Molecular Simulation Toolkit. *Bioinformatics* **2013,** *29*, 845-854.

(30) Leontiadou, H.; Mark, A. E.; Marrink, S. J. Molecular Dynamics Simulations of Hydrophilic Pores in Lipid Bilayers. *Biophys. J.* **2004,** *86*, 2156-2164.

(31) Sun, D. L.; Forsman, J.; Woodward, C. E. Amphipathic Membrane-Active Peptides Recognize and Stabilize Ruptured Membrane Pores: Exploring Cause and Effect with Coarse-Grained Simulations. *Langmuir* **2015,** *31*, 752-761.

(32) Hoover, W. G. Canonical Dynamics: Equilibrium Phase-Space Distributions. *Phys. Rev. A* **1985,** *31*, 1695-1697.

(33) Nosé, S. A. A Molecular Dynamics Method for Simulations in the Canonical Ensemble. *Mol. Phys.* **1984,** *52*, 255-268.

(34) Parrinello, M.; Rahman, A. Polymorphic Transitions in Single Crystals: A New Molecular Dynamics Method. *J. Appl. Phys.* **1981,** *52*, 7182-7190.

(35) Essmann, U.; Perera, L.; Berkowitz, M. L.; Darden, T.; Lee, H.; Pedersen, L. G. A Smooth Particle Mesh Ewald Method. *J. Chem. Phys.* **1995,** *103*, 8577-8593.

(36) Piana, S.; Lindorff-Larsen, K.; Dirks, R. M.; Salmon, J. K.; Dror, R. O.; Shaw, D. E. Evaluating the Effects of Cutoffs and Treatment of Long-Range Electrostatics in Protein Folding Simulations. *PLoS ONE* **2012,** *7*, e39918.

(37) Berendsen, H. J. C.; Postma, J. P. M.; van Gunsteren, W. F.; DiNola, A.; Haak, J. R. Molecular Dynamics with Coupling to An External Bath. *J. Chem. Phys.* **1984,** *81*, 3684-3690.

(38) Sun, D. L.; Forsman, J.; Woodward, C. E. Evaluating Force Fields for the Computational Prediction of Ionized Arginine and Lysine Side-Chains Partitioning into Lipid Bilayers and Octanol. *J. Chem. Theory Comput.* **2015,** *11* (4), 1775-1791.

(39) Hub, J. S.; de Groot, B. L.; Grubmüller, H.; Groenhof, G. Quantifying Artifacts in Ewald Simulations of Inhomogeneous Systems with a Net Charge. *J. Chem. Theory Comput.* **2014,** *10*, 381-390.

(40) Kučerka, N.; Nagle, J. F.; Sachs, J. N.; Feller, S. E.; Pancer, J.; Jackson, A.; Katsaras, J. Lipid Bilayer Structure Determined by the Simultaneous Analysis of Neutron and X-ray Scattering Data. *Biophys. J.* **2008,** *95*, 2356-2367.

(41) Upadhyay, S. K.; Wang, Y.; Zhao, T.; Ulmschneider, J. P. Insights from Micro-Second Atomistic Simulations of Melittin in Thin Lipid Bilayers. *J. Membr. Biol.* **2015,** *DOI: 10.1007/s00232-015-9807-8*.

(42) Gordon-Grossman, M.; Gofman, Y.; Zimmermann, H.; Frydman, V.; Shai, Y.; Ben-Tal, N.; Goldfarb, D. A Combined Pulse EPR and Monte Carlo Simulation Study Provides Molecular Insight on Peptide-Membrane Interactions. *J. Phys. Chem. B* **2009,** *113*, 12687-12695.

(43) Karal, M. A.; Alam, J. M.; Takahashi, T.; Levadny, V.; Yamazaki, M. Stretch-Activated Pore of the Antimicrobial Peptide, Magainin 2. *Langmuir* **2015,** *31*, 3391-3401.

(44) Huang, H. W.; Chen, F. Y.; Lee, M. T. Molecular Mechanism of Peptide-Induced Pores in Membranes. *Phys. Rev. Lett.* **2004,** *92*, 198304.

(45) Tieleman, D. P.; Marrink, S. J. Lipids out of Equilibrium: Energetics of Desorption and Pore Mediated Flip-Flop. *J. Am. Chem. Soc.* **2006,** *128*, 12462-12467.

(46) Huang, K.; García, A. E. Effects of Truncating van der Waals Interactions in Lipid Bilayer Simulations. *J. Chem. Phys.* **2014,** *141*, 105101.

(47) Fattal, E.; Nir, S.; Parente, R. A.; Szoka, F. C. Pore-Forming Peptides Induce Rapid Phospholipid Flip-Flop in Membranes. *Biochemistry* **1994,** *33*, 6721-6731.

(48) Matsuzaki, K.; Murase, O.; Fuji, N.; Miyajima, K. An Antimicrobial Peptide, Magainin 2, Induced Rapid Flip-Flop of Phospholipids Coupled with Pore Formation and Peptide Translocation. *Biochemistry* **1996,** *35*, 11361-11368.

(49) Anglin, T. C.; Brown, K. L.; Conboy, J. C. Phospholipid Flip-Flop Modulated by Transmembrane Peptides WALP and Melittin. *J. Struct. Biol.* **2009,** *168*, 37-52.

(50) Mihajlovic, M.; Lazaridis, T. Antimicrobial Peptides Bind More Strongly to Membrane Pores. *Biochim. Biophys. Acta Biomembr.* **2010,** *1798*, 1494-1502.

(51) Leveritt, J. M.; Pino-Angeles, A.; Lazaridis, T. The Structure of a Melittin-Stabilized Pore. *Biophys. J.* **2015,** *108*, 2424-2426.

(52) Drin, G.; Antonny, B. Amphipathic Helices and Membrane Curvature. *FEBS Lett.* **2010,** *584*, 1840-1847.

(53) Wimley, W. C.; White, S. H. Experimentally Determined Hydrophobicity Scale for Proteins at Membrane Interfaces. *Nat. Struct. Biol.* **1996,** *3*, 842-848.

(54) Huang, H. W. Free Energies of Molecular Bound States in Lipid Bilayers: Lethal Concentrations of Antimicrobial Peptides. *Biophys. J.* **2009,** *96*, 3263-3272.

(55) Evans, E.; Heinrich, V.; Ludwig, F.; Rawicz, W. Dynamic Tension Spectroscopy and Strength of Biomembranes. *Biophys. J.* **2003,** *85*, 2342-2350.

(56) Shillcock, J. C.; Seifert, U. Thermally Induced Proliferation of Pores in a Model Fluid Membrane. *Biophys. J.* **1998,** *74*, 1754-1766.

(57) Tamba, Y.; Ariyama, H.; Levadny, V.; Yamazaki, M. Kinetic Pathway of Antimicrobial Peptide Magainin 2-Induced Pore Formation in Lipid Membranes. *J. Phys. Chem. B* **2010,** *114*, 12018-12026.

(58) Wiedman, G.; Herman, K.; Searson, P.; Wimley, W. C.; Hristova, K. The Electrical Response of Bilayers to the Bee Venom Toxin Melittin: Evidence for Transient Bilayer Permeabilization. *Biochim. Biophys. Acta Biomembr.* **2013,** *1828*, 1357-1364.

(59) Giménez, D.; Sánchez-Muñoz, O. L.; Salgado, J. Direct Observation of Nanometer-Scale Pores of Melittin in Supported Lipid Monolayers. *Langmuir* **2015,** *31* (10), 3146-3158.

(60) Last, N. B.; Schlamadinger, D. E.; Miranker, A. D. A Common Landscape for Membrane-Active Peptides. *Protein Sci.* **2013,** *22*, 870-882.

(61) Fuertes, G.; Giménez, D.; Esteban-Martín, S.; Sánchez-Muñoz, O. L.; Salgado, J. A Lipocentric View of Peptide-Induced Pores. *Eur. Biophys. J* **2011,** *40*, 399-415.